

Spectral Band and Detector Optimization for Atmospheric Sounding Interferometers¹

John P. Kerekes and Héctor J. Jiménez-González

Lincoln Laboratory, Massachusetts Institute of Technology
244 Wood St., Lexington, Massachusetts, 02173 USA

ABSTRACT

In the specification and selection of spectral bands and detectors for optical remote sensing instruments, important consideration must be given to the primary scientific applications of the data. In this study, the line-by-line atmospheric code FASCOD and a Lincoln-developed detector model are used to identify the spectral band extent and peak location for $Hg_{1-x}Cd_xTe$ detector responsivity that result in the highest sounding sensitivity to atmospheric temperature and water vapor. The goal of this work was to minimize the background photon level that contributes to noise by reducing the spectral band extent and to relocate the peak detector response to the spectral region of greatest interest. An optimization score for each wavelength was computed as the product of terms accounting for sensitivity to the parameter of interest (temperature or water vapor) and insensitivity to the other, normalized by the product of the detector noise and the vertical height of the atmospheric contribution function. By examining the optimization score as a function of wavelength, reduced spectral coverage was seen to be possible without sacrificing sounding sensitivity. These reductions, along with the movement of the detector peak to above the spectral band low wavenumber edge, allowed an improvement of 15 to 33% in noise level and 10 to 15% in sounding performance as compared to the original specification.

INTRODUCTION

Data collected by infrared atmospheric sounders aboard low Earth orbiting satellites are used to compute atmospheric temperature and water vapor profiles for use in weather prediction and climate monitoring (Isaacs, et al. 1986). Current instruments are based on 1970's technology and while they provide useful data, it is widely believed that implementation of new technology would result in an improvement in weather forecasting accuracy. An example of this new technology is a Michelson interferometer that has been proposed (U. Wisconsin and Hughes, 1991) for the next generation of operational polar orbiting environmental satellites.

As part of an effort to investigate the proposed ITS design, it was decided to study possible improvements in performance through optimization of the spectral bands and detector characteristics. This paper presents the methodology adopted for this optimization and the results obtained in reducing instrument noise and in improving atmospheric profile retrievals.

OPTIMIZATION METHODOLOGY

The primary use of satellite infrared sounder data is the inference of atmospheric temperature and water vapor profiles through the application of an inverse algorithm to a spectral radiance measurement. Desirable characteristics of this measurement include sensitivity to changes in the underlying profiles, the ability to resolve vertical structure and small measurement noise. The optimization proceeded as follows.

The first step was to identify the pressure level p^* at which the contribution function $C_n(p)$ peaks for all possible spectral channels n . This function describes the relative contribution of the atmosphere to the total radiance as a function of pressure. The optimal channels and regions are found for each pressure level by comparing the optimization score (defined below) for only those channels whose contribution function peaks at that particular pressure level. The contribution function was calculated using FASCOD3P (Clough, et al., 1988) for all spectral channels n with the following formula given radiance B and transmittance τ as functions of pressure p .

$$C_n(p) = B_n(p) (d\tau_n / dp) \quad (1)$$

¹This work was sponsored by the National Oceanic and Atmospheric Administration under Air Force Contract F19628-90-C-0002.

The contribution function is also used to compute an approximate width Z_n by calculating the altitude difference between the half-maximum points. Channels with narrow widths are weighted more heavily.

FASCOD3P was also used to compute the change in atmospheric spectral radiance ΔR_n given a 5 K change in temperature or a 50% change in water vapor mixing ratio at each atmospheric level. Channels with a large radiance sensitivity to changes in temperature but a small sensitivity due to water vapor changes received more weighting as temperature channels; vice versa for water vapor channels.

The spectral radiance changes used in calculating the sounding sensitivity were then normalized by the product of detector D^* and the spectral bandwidth for each spectral band. This formulation was adopted for the purpose of the optimization study since this product is inversely proportional to the detector noise as all other noise factors were constant.

The temperature optimization score S_{nk} was computed as follows for all spectral channels n whose contribution function peaked at pressure level k .

$$S_{nk} = |\Delta R_n(\Delta t_k)| \times \quad ; \text{change in radiance due to change in temperature } t \text{ at pressure level } k$$

$$D^* \Delta v \times \quad ; \infty 1/\text{noise}$$

$$\frac{1}{\sum_{m=1}^K \frac{|\Delta R_n(\Delta q_m)|}{R_n}} \times \quad ; \text{insensitivity to changes in water vapor } q \text{ at all levels}$$

$$1/Z_n \quad ; \text{inverse width of contribution function} \quad (2)$$

A similar score is computed for water vapor by interchanging the temperature and water vapor parameters.

DETECTOR MODELS

The interferometer design uses both photoconductive (PC) and photovoltaic (PV) detectors as shown in Table 1.

TABLE 1. Original spectral band definition and detector types.

Band	Spectral Band	Detector Type
Longwave	620 - 1150 cm^{-1}	PC
Midwave	1210 - 1740 cm^{-1}	PV
Shortwave	2150 - 2720 cm^{-1}	PV

In modeling the PC detector a one-dimensional linear approximation (Rittner, 1956) is applied to n-type $Hg_{1-x}Cd_xTe$. Empirical expressions for the semiconductor parameters have been used wherever possible (Landolt, 1982, 1987). The expression for Auger recombination time is obtained from a Kane-theory calculation (Gel'mont, 1978). In addition to the g-r and Johnson noise contributions a 4 nV/ $\sqrt{\text{Hz}}$ amplifier noise has been included. The contribution of 1/f noise has been omitted. This contribution can be minimized with appropriate electronic filters. The PV model also used $Hg_{1-x}Cd_xTe$ and followed the approach of Long, 1977 and Reine, et al., 1981.

In background limited detectors it is desirable to reduce the spectral band extent so as to reduce the incident background photon flux and improve the D^* . This is the case for both the midwave and shortwave detectors. The longwave detector is limited by thermal g-r noise at the operational temperature of 90K.

The performance and spectral coverage of a detector can be traded-off by adjusting its Cd concentration x . Increasing x reduces thermal g-r noise by increasing the bandgap energy and thus the cutoff wavenumber.

Originally, the x concentrations were chosen for the best detectivity at the low wavenumber edge of the spectral bands. After review of the sounding optimization scores (described below), the concentrations were optimized to provide the best detectivity at the wavenumber of most use in the sounding application. This is desirable due to the improvement in peak detectivity obtained as the cutoff wavenumber is raised.

SOUNDING CHANNEL CHARACTERISTICS

The contribution functions, radiance sensitivities and resulting optimization scores were computed for all possible spectral channels spaced 0.01 cm^{-1} within the bands defined in Table 1. The calculations were performed at line-by-line resolutions using FASCOD3P and interpolated to 0.01 cm^{-1} , after which an unapodized interferometer spectral response was applied through a FFT and inverse FFT sequence. The calculations were performed for two mean atmospheric conditions: summer midlatitude and winter midlatitude.

Figures 1 and 2 show the peak pressure and width of the contribution functions for all channels using the summer atmosphere. The results were similar for the winter atmosphere.

OPTIMAL RESULTS

For each atmospheric temperature and water vapor pressure level, the 100 channels with the best optimization score were selected. These were then further winnowed by selecting the best five channels at each level. In many cases, optimal channels for similar levels were spaced closer than the spectral bandwidth. These "duplicates" were removed from the optimal list.

Figure 3 shows the resulting optimal channel sets for both temperature and water vapor, as well as for the two atmospheric conditions. While it is known that the longwave (as well as shortwave) band has some sensitivity to water vapor, it was decided to optimize the midwave band using only water vapor results and the long and shortwave bands using only the temperature results.

After reviewing these results it was decided to recommend the band definitions shown in Table 2. In selecting these bands consideration was also given to ozone and cloud applications.

TABLE 2. Optimized spectral band definition and wavenumber ν chosen for optimization

Band	Spectral Band	Optimized ν
Longwave	620 - 1095 cm^{-1}	700 cm^{-1}
Midwave	1210 - 1540 cm^{-1}	1300 cm^{-1}
Shortwave	2150 - 2450 cm^{-1}	2200 cm^{-1}

These spectral band definitions were chosen by considering the extent of the optimal channels within each band, as well as a desire to provide the best detector performance across spectral regions that provide sounding information about the entire atmosphere. Also, the nature of detectivity curves suggest that one desires the detector D^* peak to be at as high a wavenumber as possible since this provides the best peak detectivity. Thus, in particular, the longwave band peak location was moved to a higher wavenumber to provide good performance throughout the atmosphere. *Note:* these results are for a polar orbiting sounder and its global weather prediction role; a geosynchronous sounder with its primary role being severe weather monitoring may be designed by moving the longwave detector peak to an even higher wavenumber since the stratospheric channels around 667 cm^{-1} would not need as good noise performance.

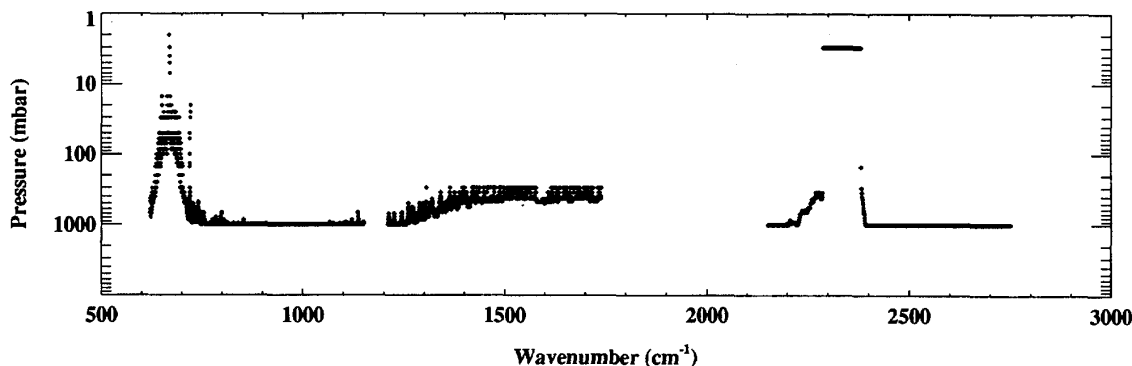


Figure 1.
Pressure at peak of contribution function for all possible channels.

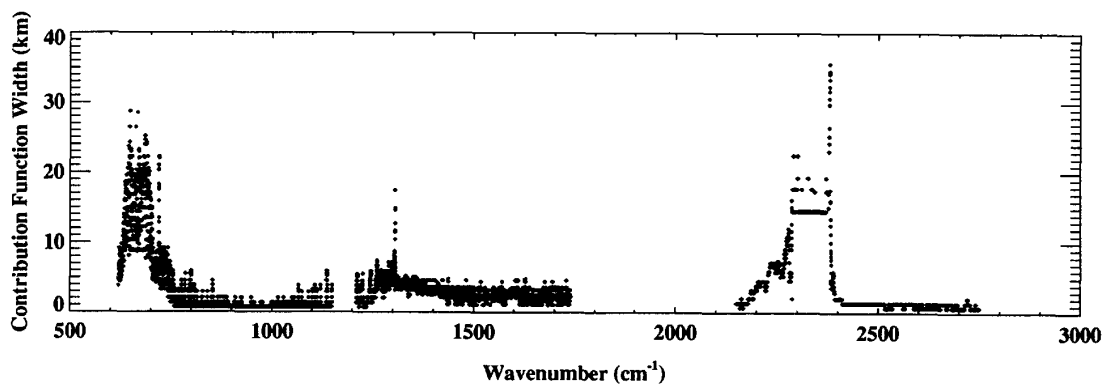


Figure 2.
Width of contribution function for all possible channels.

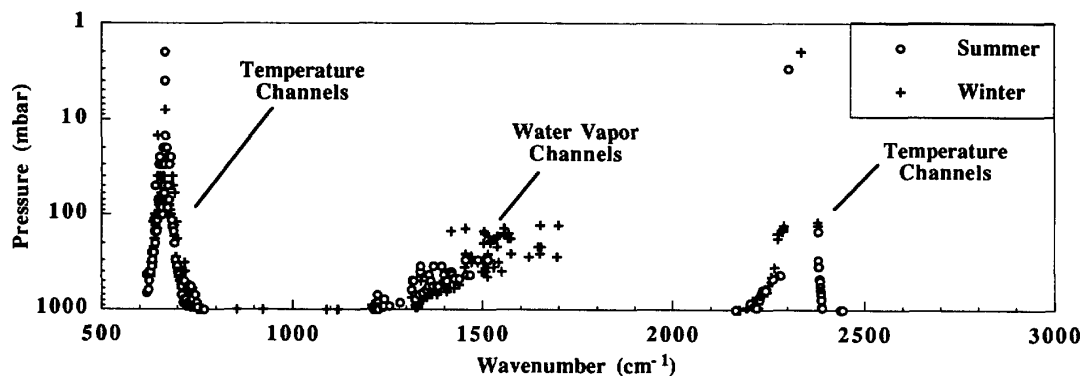


Figure 3. Optimal channels at each pressure level for Summer and Winter atmospheres.

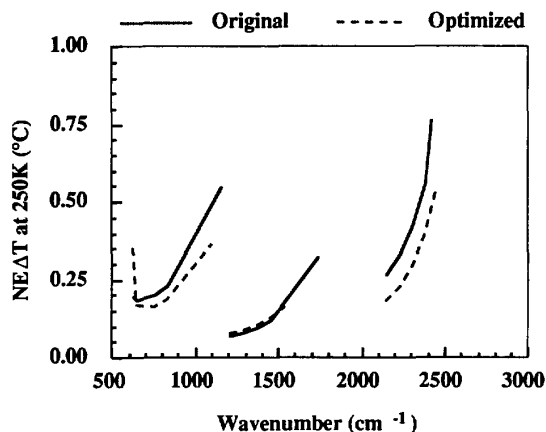


Figure 4. Impact on NEAT of spectral band and detector optimization.

Figure 4 shows predicted noise equivalent delta temperatures (NEAT's) for the original and optimized spectral bands. As can be seen, at the desired detector peaks of Table 2 the optimized design leads to improvements of 15% in the longwave, minimal in the midwave and 33% in the shortwave spectral band.

RETRIEVAL ERROR ANALYSIS

While improvements in instrument measurement noise are desirable, the real measure of utility is impact on the ultimate use of the data: the retrieval of atmospheric profiles. A linear error analysis (Kerekes, 1993) was applied to investigate the impact on retrieval error of the optimization results. The summer and winter optimal channel sets and the optimized noise levels were applied to both the summer and winter atmospheres and the results averaged. Comparison was then made to analyses using the original noise levels and a channel set obtained from uniformly spaced wavenumbers across the original spectral bands.

Table 3 shows the results of these analyses. The vertical "resolutions" were obtained by calculating the altitude differences between the peak and the first zero-crossing of the error correlation matrix obtained from the error analysis.

SUMMARY AND CONCLUSIONS

An approach to the optimization of spectral bands and detectors for infrared atmospheric sounders has been presented. The technique uses line-by-line atmospheric radiative transfer and detector models to calculate an optimization score for all candidate channels. These scores are then used to define the spectral band and detector peak wavenumber. While improvements in noise and resulting retrieval error are modest after the optimization, the methodology does provide a rational basis for instrument design.

TABLE 3. Linear error analysis results for atmospheric parameters.

Profile Parameter	Original	Optimized	Improvement
Average RMS Temperature Error (1000 - 10 mbar)	1.0 K	0.9 K	10%
Average RMS Rel. Humidity Error (1000 - 300 mbar)	15.2%	13.7%	10%
Average Temp. Vertical Resolution (1000 - 100 mbar)	1.5 km	1.2 km	15%
Average Water Vap. Vertical Resolution (1000 - 300 mbar)	1.8 km	1.6 km	10%

REFERENCES

- Clough, S.A., et al., "FASCOD3: Spectral Simulation," in Proceedings of International Radiation Symposium, 1988, pp. 372-375.
- Gel'mont, B.L., Zh. Eksp. Theor. Fiz. 75, 1978, p. 536. [Sov. Phys. JETP, 48, 1978, p. 268]
- Isaacs, R.G., Hoffman, R.N., and Kaplan, L.D., "Satellite remote sensing of meteorological parameters for global numerical weather predictions." *Reviews of Geophysics*, vol. 24, no. 4, (1986): 701-743.
- Kerekes, J.P. *A Retrieval Error Analysis Technique for Passive Infrared Atmospheric Sounders*. Technical Report 978, Lincoln Laboratory, Massachusetts Institute of Technology, Lexington, Massachusetts, 8 July 1993.
- Landolt, H., in *Numerical Data and Functional Relationships in Science and Technology*, edited by O. Madelung, vols. 17b and 22a, Springer-Verlag, Berlin, 1982, 1987.
- Long, D., *Topics in Applied Physics Vol. 19: Optical and Infrared Detectors*, edited by R.J. Keyes, Springer-Verlag, New York, 1977, p. 101.
- Reine, M.B, A.K. Sood, and T. Tredwell, in *Semiconductors and Semimetals*, edited by R. K. Willardson and A.C. Beer, vol. 18, Academic Press, New York, 1981, p. 201.
- Rittner, L.S., in *Photoconduct. Conf.*, edited by R. Breckenridge, B. Russell, and Z. Hautz, Wiley, New York, 1956, p. 2175.
- University of Wisconsin Space Science Engineering Center and Hughes Santa Barbara Research Center, *Interferometer Thermal Sounder (ITS): Feasibility Study, Final Report*, December 1991.